

# MAGNETIC FIELD EVALUATION OF AN OCTUPOLE TYPE CERAMICS CHAMBER WITH INTEGRATED PULSED MAGNET FOR BEAM INJECTION

Y. Lu\*, The Graduate University for Advanced Studies (SOKENDAI), [240-0193] Hayama, Japan  
 C. Mitsuda, H. Takaki, Y. Kobayashi, T. Uchiyama, T. Nogami  
 High Energy Accelerator Research Organization (KEK), [305-0801] Tsukuba, Japan

## Abstract

An air-core pulsed magnet named Ceramics chamber with integrated Pulsed Magnet (CCiPM) was developed as a fast dipole kicker at first. Because of its flexibility of the magnetic field, an octupole-like magnetic field can also be generated. A prototype of an octupole type CCiPM was fabricated for electron beam injection at KEK Photon Factory (KEK-PF). The DC and pulsed magnetic fields of the octupole type CCiPM were measured. Some measurement subjects of eddy-current magnetic field evaluation and background noise treatment around zero approximate magnetic field region at the center of the magnet are discussed.

## INTRODUCTION

Pulsed multipole magnet injection is being continuously developed at KEK-Photo Factory (KEK-PF). Because of the nature of multipole magnetic field, the magnet provides a strong off-axis kick effect which kick the injection beam into the storage ring acceptance and does not disturb the stored beam at the center. However, the magnet is excited by an approximate half-sinusoid current with  $1.2 \mu\text{s}$  based on the physical design [1]. Because of the eddy current effect of the iron-core, irregular magnetic field is present at the center and can induce the stored beam oscillation [2].

To realize a transparent injection, air-core pulsed magnet is a better choice for the application in future light source. An air-core pulsed magnet named Ceramics chamber with integrated Pulsed Magnet (CCiPM) has been developed as a fast dipole kicker [3]. The CCiPM can also generate an octupole-like magnetic field by adjusting the current direction. The cross-section view of the CCiPM with magnetic flux is shown in Fig. 1. The bore diameter is 40 mm, and the thickness of the ceramic chamber is 10 mm. We have proposed the design and fabricated the octupole type CCiPM [4].

The DC and pulsed magnetic fields of the octupole type CCiPM were measured. The measurement results are presented, and some measurement subjects of eddy-current magnetic field evaluation and background noise treatment around zero approximate magnetic field region at the center of the magnet are discussed.

## MAGNETIC FIELD MEASUREMENT

The model of the CCiPM is shown in Fig. 2. The coordinate is marked to illustrate the measurement result. The

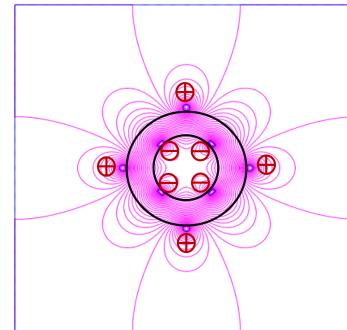


Figure 1: Cross-section view of the CCiPM with magnetic flux.

origin of the coordinate is located at the center. Some basic parameters of the CCiPM are summarized in Table 1.

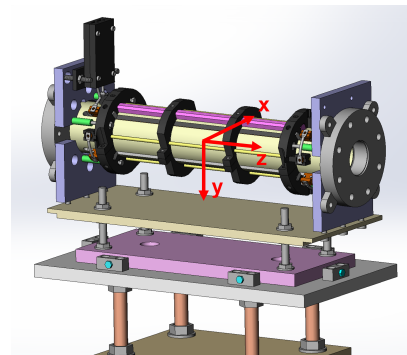


Figure 2: Model of the octupole type CCiPM.

Table 1: Basic Parameters of the CCiPM

Item	Parameter
Total length	399.4 mm
Length of the ceramic chamber	357.0 mm
Thickness of the ceramic	10.0 mm
Length of the coil embedded in the ceramic	324.0 mm
Inductance	1.45 $\mu\text{H}$
Weight	<6 kg

\* yaolu@post.kek.jp

### Measurement Principle

The DC magnetic field was measured with a Hall probe. (F.W. Bell company, model: STF99-04-02, item number: 129937). In the measurement, the current was 15 A to prevent the magnet from overheating.

As for the pulsed magnetic field, a compact pick-up probe has been developed to measure the pulsed magnetic field precisely with a 3.2 mm × 5.8 mm coil [2]. The supplied current was a half-sine shape current with a 0.8 μs pulse width, and the peak value was 200 A. In the measurement, the induced voltage  $V$  in the coil of the probe can be expressed as

$$V(t) = -\frac{d\phi}{dt} = -\frac{d}{dt} N \iint_S \mathbf{B} \cdot \mathbf{n} dS \quad (1)$$

where  $N$  is the number of turns,  $\mathbf{B}$  is the magnetic field,  $\mathbf{n}$  is the normal unit vector of the area, and  $S$  is the area of the coil.

In the measurement, the coil is fixed to be perpendicular to the magnetic field direction. Then the induced voltage is calculated as

$$V(t) = -\frac{d}{dt} N \iint_S B_0 \sin \omega t dS = -\frac{d}{dt} (B_0 S_{total} \sin \omega t) \quad (2)$$

where  $B_0$  is the peak pulsed magnetic field value,  $\omega$  is the angular frequency of the half-sine current, and  $S_{total}$  is the total effective area. The total effective area of the probe is 40.88 mm<sup>2</sup>. If the voltage signal  $V(t)$  is integrated, the peak value of the integral signal  $F_m$  corresponds to the peak pulsed magnetic field which is given by

$$B_0 = \frac{F_m}{S_{total}} \quad (3)$$

### Measurement Results

For the convenience of comparison, the DC and pulsed magnetic fields are normalized under the condition of a 3000 A current. Because of the narrow bore of the CCiPM and thickness of the measurement arm, the horizontal measurement region was limited, which was from  $x=-12$  mm to 12 mm. In the measurement, the step size in the  $x$  direction is 1 mm, and it is 2 mm in the  $z$  direction.

The comparison of the horizontal magnetic field distribution at the center is shown in Fig. 3. The result of DC magnetic field is almost same with the simulation data. However, the off-axis pulsed magnetic field is smaller than 20% of the simulation value.

Figure 4 shows the comparison of the longitudinal magnetic field distribution at  $x=10$  mm ( $y=0$  mm,  $-300 \leq z \leq 300$  mm). The shape of the DC magnetic field distribution is almost same with the simulation. As for the pulsed magnetic field, it is still less than the simulation. At  $z=0$  mm, the simulation value, the normalized DC magnetic field, and the normalized pulsed magnetic field are 0.0140 T, 0.0138 T, 0.0114 T, respectively.

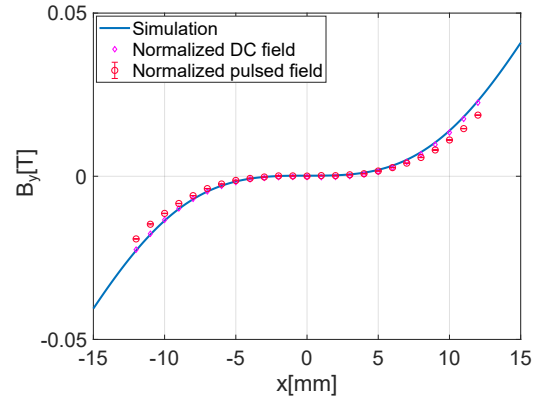


Figure 3: Comparison of the horizontal distribution at the center.

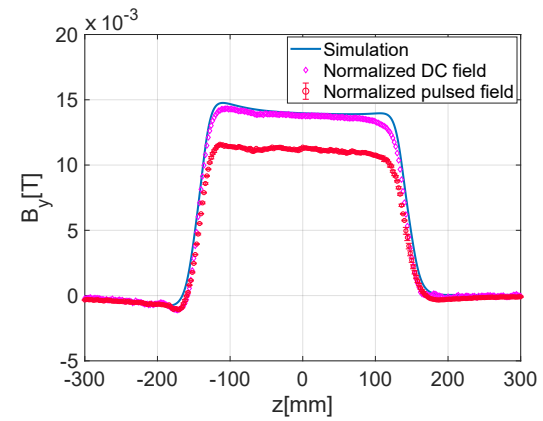


Figure 4: Comparison of the longitudinal distribution at  $x=10$  mm ( $y=0$  mm,  $-300 \leq z \leq 300$  mm).

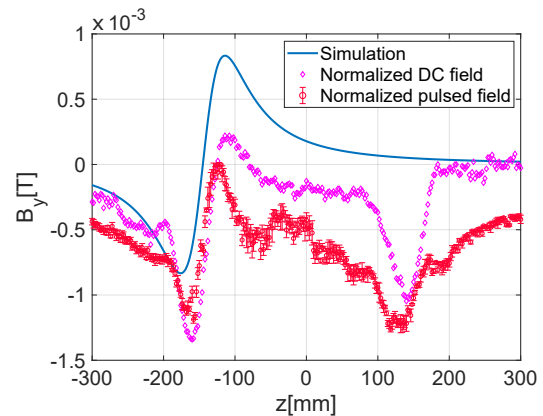


Figure 5: Comparison of the longitudinal distribution at  $x=0$  mm ( $y=0$  mm,  $-300 \leq z \leq 300$  mm).

Finally, the longitudinal magnetic field distributions at  $x=0$  mm ( $y=0$  mm,  $-300 \leq z \leq 300$  mm) are shown in Fig. 5. Compared with the simulation, two spikes in the DC magnetic field distribution appears around  $z=\pm 150$  mm. It indicates that some undesirable magnetic components may present in the prototype. As for the pulsed magnetic field, there is a problem about the electromagnetic noise which

cannot be removed totally in the circuit. Therefore, there is an offset of the magnetic field at  $z=300$  mm where the DC magnetic field is equal to zero. Although the measurement result has a systematic error, the distribution of the normalized pulsed magnetic field is similar with that of the normalized DC magnetic field. Two spikes also appears around  $z=\pm 150$  mm, which can prove the presence of an irregular magnetic field.

## ISSUES IN THE DC MAGNETIC FIELD MEASUREMENT

According to the result of the DC magnetic field, the main problem is the undesirable magnetic field at the center. The possible reason is discussed in this section.

### *The Kovar between the Ceramic and Flange*

Because CCiPM is an air-core magnet, the magnetic field is only generated from the current in the coil. There is no magnetic component in the simulation model. However, the joint between the flange and ceramic is made from Kovar, which is a magnetic material. As shown in Fig. 6, the Kovar is located at the end of the CCiPM. In Fig. 5, the distribution of the Normalized DC magnetic field has two spikes around  $z=\pm 150$  mm. According to the design, the full length of the CCiPM is 400 mm, and the Kovar at one end is located at  $z=-180$  mm.

In Fig. 5, the normalized DC magnetic field at  $z=180$  mm is almost zero, but the spike appears at  $z=150$  mm. Therefore, the spike cannot be induced by the Kovar.

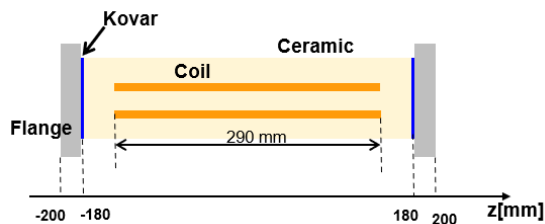


Figure 6: Schematic view of the CCiPM.

### *Alignment and Manufacturing Errors of the Arc Conductor*

One element that may produce undesirable magnetic field is the arc conductor which is used to change the current direction. The arc conductor has manufacturing errors. Therefore, the current flow in the arc conductor is not symmetric, and the magnetic field at the center cannot be compensated to be almost zero. To reduce the magnetic field error of the arc conductor, the laser level was used to align the position of the copper conductor. The photograph of the arc conductor is shown in Fig. 7. In addition, the arc conductor was randomly assembly for several times to measure the longitudinal magnetic field distribution at  $x=0$  mm. The magnetic field strength hardly changes. Therefore, the spike in the longitudinal distribution is not caused by the arc conductor.

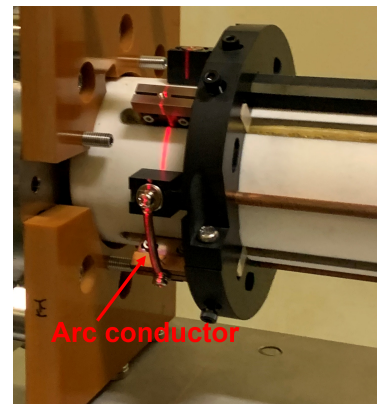


Figure 7: Photograph of the arc conductor in the CCiPM.

### *The Joint between the Metal Block and Coil*

Figure 8 shows the CCiPM's joint for the lead wire. The metal block and coil are brazed together. The arc conductor is fixed on the metal block by the bolt, which has a strong mechanical strength. In the simulation, the current density is assumed to be uniform in the metal block. In a real model, the direction of the current flow and current density depend on the quality of the brazing. The position of the joint is located at  $z=\pm 145$  mm, which is near the position of the spike. Therefore, the uniformity of the magnetic field may be influenced by the joint.

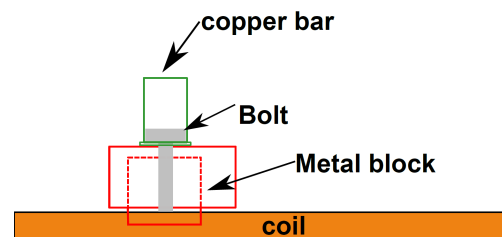


Figure 8: Schematic view of the CCiPM's joint for the lead wire.

## ISSUES IN THE PULSED MAGNETIC FIELD MEASUREMENT

There are two issues in the pulsed magnetic field measurement. One is the off-axis magnetic field is smaller than 20% of the designed value, the other one is the accuracy of measuring the magnetic field at the center.

### *Eddy Current Medium in the Measurement*

Some eddy current mediums may have effects on the pulsed magnetic field measurement. The CCiPM is an air-core magnet, and the jig is made from resin. The conductive components in the measurement are the titanium coating inside the chamber and alignment stage made from stainless steel. According to the former simulation result, the reduction ratio of magnetic field induced by the coating is less than 1% [4]. Then the eddy current effect of the stainless steel was evaluated in the ELF/MAGIC [5].

As shown in Fig. 9, a simple model was constructed. The vertical distance between the midplane of the CCI<sub>PM</sub> and stainless steel stage is 90 mm. Although the eddy-magnetic field is present around the stage, the magnetic field in the midplane of the CCI<sub>PM</sub> does not change. Therefore, it is considered that eddy-current magnetic field does not affect the pulsed magnetic field in the measurement.

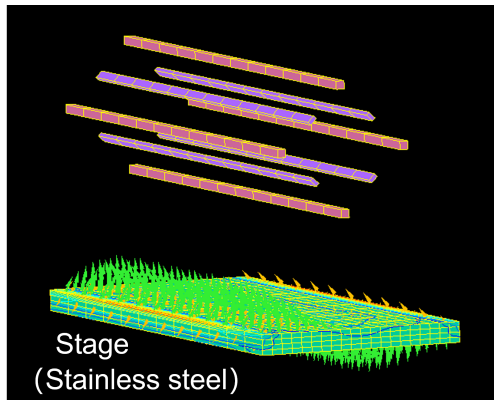


Figure 9: Magnetic flux generated by the eddy current of the stage.

### Limitation of the Resolution Power of the Probe

The measurement precision for measuring a weak pulsed magnetic field is limited by the resolution level of the probe. The electromagnetic noise disturbs the measurement circuit. To reduce the noise in the measurement, the cable was twisted together and fed into a aluminum tube that can shield against high-frequency magnetic field. However, the noise cannot be removed totally. When the probe measured a zero-magnetic field region outside the magnet, the integrated voltage signal had a noise signal with a 1.2 nV·s maximum amplitude, which was a systematic error in the measurement. After calculation by Eq. 3, the noise level is  $2.9 \times 10^{-5}$  T. Hence, the probe cannot measure a pulsed magnetic field clearly whose peak value is smaller than  $2.9 \times 10^{-5}$  T. After the normalization, the value becomes  $4.4 \times 10^{-4}$  T. Because the magnetic field is too weak at the center of the CCI<sub>PM</sub>, a clear integrated voltage signal with a half-sine wave shape was not measured at the center.

### The Ringing of the Output Current Signal.

Although a noise signal with an amplitude of 1.2 nV·s disturbed the measurement at the center, it is not likely to be related to the off-axis magnetic field measurement. Because at  $x=12$  mm ( $y=0$  mm,  $z=0$  mm), the peak value of the integrated voltage signal could reach 50 nV·s. the influence of the noise is less than 2.4%. In the experiment, the calculated pulsed magnetic field is smaller than 20% of the simulation value.

To figure out this issue, the integrated voltage signal is compared with the current signal of the Current Transformer (CT), which is shown in Fig. 10. The CT signal is not identical to the integrated voltage signal. Because of the small

inductance of the CCI<sub>PM</sub>, the pulse width is 0.8 μs. Owing to the performance of the power source, the output current is not a half-sine wave shape, It represents that the magnetic field pulse is not a half-sine wave shape. Therefore, the calculation of the peak magnetic field is badly affected. The result also shows that the pick-up probe is not capable of reconstructing a signal induced by an external pulsed magnetic field whose pulse width is smaller than 1 μs. Consequently, the ringing of the current signal is the most likely cause of the problem in the off-axis pulsed magnetic field measurement. To suppress the ringing of the current signal, an impedance load should be added in the circuit to match the power source.

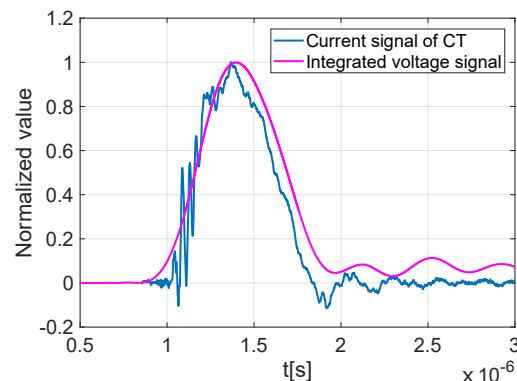


Figure 10: Comparison between the CT signal and integrated voltage signal ( $x=12$  mm,  $y=0$  mm,  $z=0$  mm).

## CONCLUSION

The DC and pulsed magnetic fields of the octupole type CCI<sub>PM</sub> were measured. The DC magnetic field is almost consistent with the simulation. However, there is a small irregular magnetic field in the longitudinal distribution at the center, which may increase the perturbation on the stored beam. It is highly possible that the problem is caused by the joint between the coil and metal block. The brazing part will be investigated carefully in the future.

As for the pulsed magnetic field measurement, the eddy-current magnetic field has negligible effect in the measurement. The resolution power is not enough for measuring the weak magnetic field at the center. In addition, the ringing of the output current signal disturbs the measurement circuit to obtain an accurate peak pulsed magnetic field value. To improve the current shape, the pulse width of the output current can be expanded by adding an impedance load. Furthermore, a pulsed power source whose output current has a several microseconds pulse duration can be used to improve the S/N. The main field signal is expected to be increased at the center.

## ACKNOWLEDGEMENTS

The author thanks the collaboration from KYOCERA Co. This work was supported by JSPS KAKENHI Grant number 19K2649 (Representative, C.Mitsuda).

## REFERENCES

- [1] H. Takaki *et al.*, "Beam injection with a pulsed sextupole magnet in an electron storage ring", *Phys. Rev. ST Accel. Beams* 13 (2) (2010) 020705.
- [2] Y. Lu *et al.*, "Evaluation of Eddy Current Effects on a Pulsed Sextupole Magnet by a Precise Magnetic field Measurement at KEK-PF" in *Proc. 17th Annual Meeting of Particle Accelerator Society of Japan. (PASJ'2020)*, Japan, Sep. 2020, Online.
- [3] C. Mitsuda *et al.*, "Development of the Ceramics Chamber integrated Pulsed Magnet Fitting for a Narrow Gap" in *Proc. 6th International Particle Accelerator Conf.(IPAC'15)*, Richmond, VA, USA, May. 2015, pp. 2879–2882.
- [4] Y. Lu *et al.*, "New Development of Ceramics Chamber with Integrated Pulsed Magnet for Pulsed Multipole Injection at KEK-PF" in *Proc. 18th Annual Meeting of Particle Accelerator Society of Japan. (PASJ'2021)*, Japan, Sep. 2020, Online.
- [5] <https://www.elf.co.jp/>